Self-assembly of Photofunctional Siloxane-Based Calix[4]arenes on Oxide Surfaces

Tamar van der Boom,[†] Guennadi Evmenenko,[‡] Pulak Dutta,[‡] and Michael R. Wasielewski*,[†]

Department of Chemistry and Center for Nanofabrication and Molecular Self-Assembly and Department of Physics and Astronomy and the Materials Research Center, Northwestern University, Evanston, Illinois 60208-3113

Received April 8, 2003. Revised Manuscript Received August 8, 2003

The synthesis of photofunctional calix[4]arenes and the formation and characterization of self-assembled monolayers (SAMs) made from them is described. Two identical 4-(*N*-piperidinyl)naphthalene-1,8-dicarboximide or perylene-3,4:9,10-bis(dicarboximide) chromophores were covalently attached to the upper rim of calix[4]arene at the 1- and 3-positions, whereas the lower rim was functionalized with four reactive silane groups to ensure strong, covalent multisite binding to hydrophilic oxide surfaces such as quartz and silicon wafers. This strategy allows spatially proximate chromophoric dimers to be attached to surfaces, while offering the flexibility of isolating or diluting these dimer units on the surface. Homo- and heterogeneous nanoscale thin films (1.2−2.1-nm thick) were assembled from solution and characterized using synchrotron X-ray specular reflectivity, advancing contact angle measurements, atomic force microscopy, and optical absorption and fluorescence spectroscopy. Optical spectroscopy of the films show that strong electronic interactions occur between the perylene-3,4:9,10-bis(dicarboximide) dimers, while the 4-(*N*-piperidinyl)naphthalene-1,8-dicarboximide dimers show little interaction. However, in the latter case, the solvatochromic nature of the chromophore illustrates the low-polarity environment of the films.

Introduction

The design and development of new molecular photonic materials with excellent optical, thermal, and chemical properties is a topic of much current interest.[1−4] Langmuir−Blodgett (LB) film transfer and self-assembly (SA) have been widely used to obtain structurally well-defined organic thin films (i.e., mono- and multilayers).[5−34] Chemisorptive siloxane SA has been developed by Sagiv and others[25−34] and is known to yield densely packed organic films on hydrophilic substrates. Most challenging is the development of covalently immobilized chromophores/fluorophores to prepare novel photonically robust molecular arrays directly on silicon or related substrates,[30−34] allowing facile device integration.[35−37] In particular, the need to position two or more

* To whom correspondence should be addressed. Fax: (847)-467-1425. E-mail: wasielew@chem.northwestern.edu.

[†] Department of Chemistry and Center for Nanofabrication and Molecular Self-Assembly.

[‡] Department of Physics and Astronomy and the Materials Research Center.

(1) Lukas, A. S.; Wasielewski, M. R. *Molecular Switches*; Wiley-VCH GmbH: Weinheim, 2001.

(2) Flink, S.; van Veggel, F. C. J. M.; Reinhoudt, D. N. *Adv. Mater.* **2000**, *12*, 1315−1329.

(3) Dalton, L. R. *J. Mater. Chem* **1999**, *9*, 1905−1920.

(4) Wasielewski, M. R. *Chem. Rev.* **1992**, *92*, 435−461.

(5) Schwartz, H.; Mazor, R.; Khodorkovsky, V.; Shapiro, L.; Klug, J. T.; Kovalev, E.; Meshulam, G.; Berkovic, G.; Kotler, Z.; Efrima, S. *J. Phys. Chem. B* **2001**, *105*, 5914−5921.

(6) Ricceri, R.; Neto, C.; Abbotto, A.; Facchetti, A.; Pagani, G. A. *Langmuir* **1999**, *15*, 2149−2151.

(7) Roberts, M. J.; Lindsay, G. A.; Herman, W. N.; Wynne, K. J. *J. Am. Chem. Soc.* **1998**, *120*, 11202−11203.

(8) Wijekoon, W. M. K. P.; Wijayu, S. K.; Bhawalkar, J. D.; Prasad, P. N.; Penner, T. L.; Armstrong, N. J.; Ezenyilimba, M. C.; Williams, D. J. *J. Am. Chem. Soc.* **1996**, *118*, 4480−4483.

(9) Ashwell, G. J.; Jackson, P. D.; Crossland, W. A. *Nature* **1994**, *368*, 438−440.

(10) Bakiamoh, S. B.; Blanchard, G. J. *Langmuir* **2001**, *17*, 3438−3446.

(11) Neff, G. A.; Helfrich, M. R.; Clifton, M. C.; Page, C. J. *Chem. Mater.* **2000**, *12*, 2363−2371.

(12) Flory, W. C.; Mehrens, S. M.; Blanchard, G. J. *J. Am. Chem. Soc.* **2000**, *122*, 7976−7985.

(13) Hanken, D. G.; Naujok, R. R.; Gray, J. M.; Corn, R. M. *Anal. Chem.* **1997**, *69*, 240−248.

(14) Fang, M.; Kaschak, D. M.; Sutorik, A. C.; Mallouk, T. E. *J. Am. Chem. Soc.* **1997**, *119*, 12184−12191.

(15) Katz, H. E.; Wilson, W. L.; Scheller, G. *J. Am. Chem. Soc.* **1994**, *116*, 6636−6640.

(16) Doron-Mor, H.; Hatzor, A.; Vaskevich, A.; van der Boom-Moav, T.; Shanzer, A.; Rubinstein, I.; Cohen, H. *Nature* **2000**, *406*, 382−385.

(17) Hatzor, A.; van der Boom-Moav, T.; Yochelis, S.; Vaskevich, A.; Shanzer, A.; Rubinstein, I. *Langmuir* **2000**, *16*, 4420−4423.

(18) Hatzor, A.; Moav, T.; Cohen, H.; Matlis, S.; Libman, J.; Vaskevich, A.; Shanzer, A.; Rubinstein, I. *J. Am. Chem. Soc.* **1998**, *120*, 13469−13477.

(19) Moav, T.; Hatzor, A.; Cohen, H.; Libman, J.; Rubinstein, I.; Shanzer, A. *Chem. Eur. J.* **1998**, *4*, 502−507.

(20) Bruening, M.; Cohen, R.; Guillemoles, J. F.; Moav, T.; Libman, J.; Shanzer, A.; Cahen, D. *J. Am. Chem. Soc.* **1997**, *119*, 5720−5728.

(21) Schönherr, H.; Vancso, G. J.; Huisman, B.-H.; van Veggel, F. C. J. M.; Reinhoudt, D. N. *Langmuir* **1999**, *15*, 5541−5546.

(22) Huisman, B.-H.; Thoden, v. V., E. U.; van Veggel, F. C. J. M.; Engbersen, J. F. J.; Reinhoudt, D. N. *Tetrahedron Lett.* **1995**, *18*, 3273−3276.

(23) Dermody, D. L.; Crooks, R. M.; Kim, T. *J. Am. Chem. Soc.* **1996**, *118*, 11912−11917.

(24) Cygan, M. T.; Collins, G. E.; Dunbar, T. D.; Allara, D. L.; Gibbs, C. G.; Gutsche, C. D. *Anal. Chem.* **1999**, *71*, 142−148.

(25) Ulman, A. *Chem. Rev.* **1996**, *96*, 1533−1554.

(26) Moon, J. H.; Shin, J. W.; Kim, S. Y.; Park, J. W. *Langmuir* **1996**, *12*, 4621−4624.

(27) Kurth, D. G.; Bein, T. *Langmuir* **1993**, *9*, 2965−2973.

(28) Wasserman, S. R.; Tao, Y.-T.; Whitesides, G. M. *Langmuir* **1989**, *5*, 1074−1087.

(29) Maoz, R.; Sagiv, J. *Langmuir* **1987**, *3*, 1034−1044.

(30) van der Boom, M. E.; Richter, A. G.; Malinsky, J. E.; Lee, P. A.; Armstrong, N. R.; Dutta, P.; Marks, T. J. *Chem. Mater.* **2001**, *13*, 15−17.

10.1021/cm034247h CCC: $25.00
Published on Web 09/04/2003

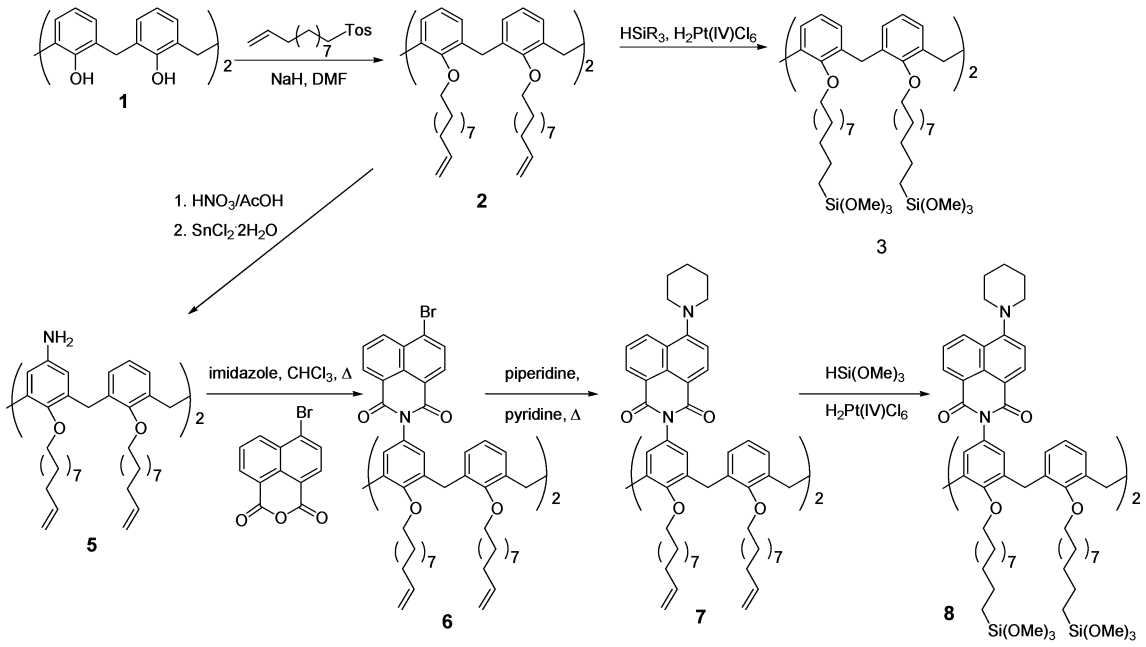

Figure 1. Synthesis of the functionalized siloxane-based calix[4]arenes scaffolds, **3** and **8**.

photoactive units at fixed orientations and distances relative to one another to ensure specific functionality, and at the same time provide for surface attachment, requires the use of a scaffold that can pre-organize the spatial relationships between the active units. In this paper, we report the synthesis of calix[4]arene molecular scaffolds that are functionalized with two side-by-side chromophores and the formation and characterization of siloxane-based monolayers from them. Thin film formation with sulfide-derivatized calix[4]arenes on gold substrates has been studied in detail by Reinhoudt and others,[21−24] while integration of siloxane-derivatized calix[4]arenes in organic thin films on transparent substrates is relatively rare.[33] We have attached two identical fluorophores to the upper rim of the calix[4]-arene at the 1- and 3-positions, while the lower rim was functionalized with four reactive silane groups to ensure strong, covalent multisite binding to various hydrophilic substrates, such as silicon, quartz, and indium tin oxide-coated glass. Key to the study and utilization of these new immobilized photonic compounds is a reliable understanding of their solid-state characteristics. Specular X-ray reflectivity (XRR), contact-mode AFM, advancing contact angle (CA) measurements, and optical absorption and fluorescence spectrometry are used in this study to quantitatively determine the density, film thickness, roughness, morphology, and optical properties of these new materials.

Results and Discussion

Synthesis of Photofunctional Siloxane-Based Calix[4]arenes. The lower rim of calix[4]arene **1** was alkylated at the 25-, 26-, 27-, and 28-positions with 10-undecen-1-yl tosylate affording **2** in the cone conformation in 80% yield as a white solid (Figure 1). In the cone conformation the oxygen atoms of all four phenyl ethers are positioned on the same side of the calix[4]arene as indicated in Figure 1. Hydrosilylation of **2** with $HSi(OMe)_3$ and a catalytic amount of $H_2Pt(IV)Cl_6{\cdot}xH_2O$ in dry CH_2Cl_2 at room temperature afforded **3** in quantitative yield. Compound **3** was characterized using conventional analytical techniques. The upper rim of **2** was nitrated using HNO_3/AcOH to give **4** followed by reduction of the nitro groups at the 15- and 17-positions to amines, yielding **5** as a white powder. Diamine **5** was condensed with 4-bromo-1,8-naphthalic anhydride affording **6** followed by nucleophilic displacement of the bromine with piperidine to give **7**. Subsequently, compound **7** was quantitatively hydrosilylated using $HSi(OMe)_3$ and $H_2Pt(IV)Cl_6{\cdot}xH_2O$ in dry CH_2Cl_2 affording **8**.

Reaction of *N*-octyl-1,7-bis-(3,5-di-*tert*-butylphenoxy)-perylene-3,4-dicarboxyanhydride-9,10-dicarboximide, **9**,[38] with compound **5** in refluxing pyridine/imidazole resulted in the formation of **10** (Figure 2).[39] Hydrosilylation of **10** with $HSi(OMe)_3$ in the presence of $H_2Pt(IV)Cl_6{\cdot}xH_2O$ in dry CH_2Cl_2 at room temperature afforded **11**.

Preparation and Characterization of Calix[4]-arene-Based Self-assembled Monolayers (SAMs). SAMs were prepared by immersing freshly cleaned hydrophilic substrates (quartz and silicon wafers) in a ~1.0 mM dry toluene solution of compounds **3** or **8** in

(31) Huang, W.; Helvenston, M.; Casson, J. L.; Wang, R.; Bardeau, J.-F.; Lee, Y.; Johal, M. S.; Swanson, B. I.; Robinson, J. M.; Li, D. Q. *Langmuir* **1999**, *15*, 6510−6514.
(32) Li, D. Q.; Swanson, B. I.; Robinson, J. M.; Hoffbauer, M. A. *J. Am. Chem. Soc.* **1993**, *115*, 6975−6980.
(33) van der Veen, N. J.; Flink, S.; Deij, M. A.; Egberink, R. J. M.; van Veggel, F. C. J. M.; Reinhoudt, D. N. *J. Am. Chem. Soc.* **2000**, *122*, 6112−6113.
(34) Chrisstoffels, L. A. J.; Adronov, A.; Fréchet, J. M. J. *Angew. Chem., Int. Ed.* **2000**, *39*, 2163−2167.
(35) van der Boom, M. E.; Malinsky, J. E.; Zhao, Y.-G.; Chang, S.; Lu, W.-K.; Ho, S.-T.; Marks, T. J. *Polym. Prepr. (Am. Chem. Soc., Div. Polym. Chem.)* **2001**, *42*, 550−551.
(36) Zhao, Y.-G.; Wu, A.; Lu, H.-L.; Chang, S.; Lu, W. K.; Ho, S. T.; van der Boom, M. E.; Marks, T. J. *Appl. Phys. Lett.* **2001**, *79*, 587−589.
(37) Lundquist, P. M.; Lin, W.; Zhao, H.; Hahn, D. N.; Yitzchaik, S.; Marks, T. J.; Wong, G. K. *Appl. Phys. Lett.* **1997**, *70*, 1941−1943.
(38) Lukas, A. S.; Zhao, Y.; Miller, S. E.; Wasielewski, M. R. *J. Phys. Chem. B* **2002**, *106*, 1299−1306.
(39) van der Boom, T.; Hayes, R. T.; Zhao, Y.; Bushard, P. J.; Weiss, E. A.; Wasielewski, M. R. *J. Am. Chem. Soc.* **2002**, *124*, 9582−9590.

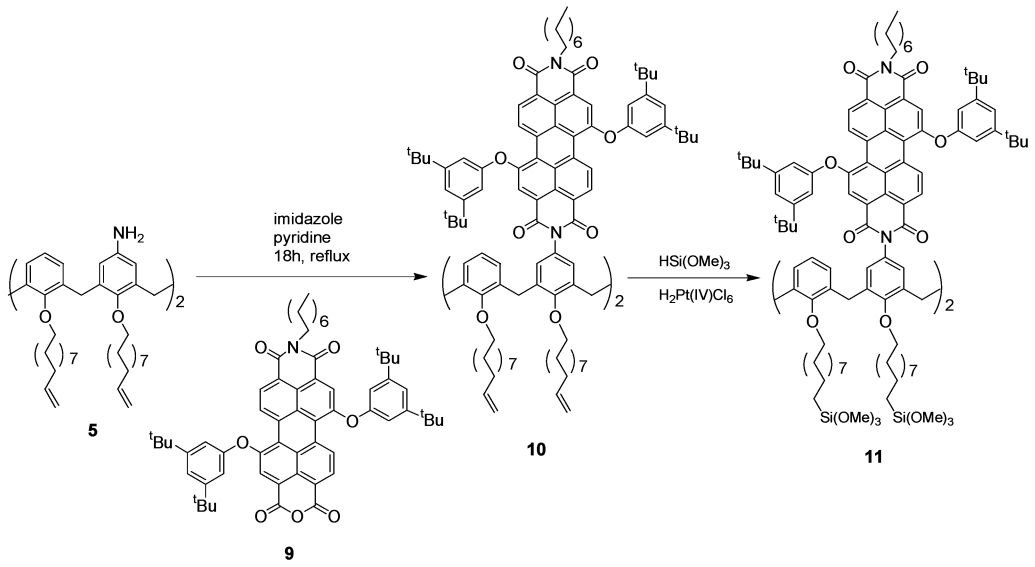

Figure 2. Synthesis of the functionalized siloxane-based calix[4]arene scaffold, **11**.

Schlenk-type reactors for 18 h at 80 °C under N_2. After cooling to room temperature, the substrates were thoroughly rinsed with dry toluene and acetone, sonicated in methanol, and dried under a stream of N_2. Mixed SAMs were prepared as well. For example, a dry CH_2Cl_2 solution of **2** and **10** (mole ratio 1:1) was quantitatively hydrosilylated using $HSi(OMe)_3$ and $H_2Pt(IV)Cl_6 \cdot xH_2O$ to afford **3** and **11**, respectively. After removal of the catalysts and all volatiles, the residue was dissolved in dry toluene. Subsequently, the heterogeneous **3**,**11**-based SAMs were prepared by immersing the substrates in the solution for 18 h at 80 °C under N_2.

The resulting structural regularity of the chemisorptive SAMs have been characterized by a full complement of physicochemical techniques. Advancing CA measurements on the functionalized substrates reveal hydrophobic surfaces with $\theta_a \sim 98°$, in accordance with the formation of densely packed organic films,[21−24] exposing only the calix[4]arene upper rim to the outer surface. The thermally stable hydrophobic films are inert to common organic solvents and cannot be removed from the surface by the standard "adhesive tape test",[40] indicating that the calix[4]arenes are covalently attached to the hydrophilic surfaces. Contact mode AFM measurements of **3** and **8**-based films ($1 \times 1\ \mu m^2$ scan area) reveal smooth, essentially featureless surfaces with an rms roughness of 9 ± 2 Å (**3**) and 12 ± 4 Å (**8**), consistent with the formation of an organic film with a high structural regularity (bare Si substrates have an rms roughness of 5 ± 2 Å).

The organic films made from **3**, **8**, and **11** were characterized extensively using X-ray reflectivity (XRR) measurements. In general, X-ray specular reflectivity is determined by the electron density profile $\rho(z)$ perpendicular to the sample surface. In the Born approximation, the normalized reflectivity is[41−43]

$$\frac{R(q_z)}{R_F(q_z)} = \left|\frac{1}{\rho_{Si}}\int \frac{\partial\rho(z)}{\partial z} e^{-izq_z}\, dz\right|^2 \qquad (1)$$

where the wave vector transfer $|q| = q_z = (4\pi/\lambda)\sin\theta$ is along the surface normal, ρ_{Si} is the electron density of the semi-infinite silicon substrate, $\rho(z)$ is the electron density distribution inside the film averaged over the in-plane coherence length of the X-rays (usually ∼1−3 μm), and $R_F(q_z)$ is the theoretical Fresnel reflectivity for an ideally sharp interface. Structural information from the XRR data can be obtained by using the Patterson function. It is known that the inverse Fourier transform on the normalized reflectivity is related to the corresponding one-dimensional Patterson function, $P(z)$:[44,45]

$$P(z) \propto \int \frac{\partial\rho(z+s)}{\partial s} \cdot \frac{\partial\rho(s)}{\partial s}\, ds \qquad (2)$$

The Patterson function is sensitive to the relative positions of interfaces in the electron density distribution and the positions of peaks in $P(z)$ correspond to the distances between regions where the density is changing rapidly. Assuming a model for electron density profile, detailed structural information can be obtained by varying model parameters and fitting the reflectivity curve. A typical model is the Gaussian-step model,[41] which assumes that the film consists of a silicon substrate and layers of different electron densities, ρ_i, with Gaussian broadened interfaces, σ_i,

$$\frac{R(q_z)}{R_F(q_z)} = \left|\sum_{i=0}^{N} \frac{(\rho_i - \rho_{i+1})}{\rho_0} e^{-iq_z D_i} e^{-q_z^2 \sigma_{i+1}^2/2}\right|^2 \qquad (3)$$

where N is the number of layers, ρ_0 is the electron density of the substrate ($=\rho_{Si}$), $D_i = \sum_{j=1}^{i} T_j$ is the distance from the substrate surface to the ith interface, and T_i is the thickness of the ith layer. The reflectivity

(40) Huang, Z.; Wang, P.-C.; MacDiarmid, A. G.; Xia, Y.; Whitesides, G. M. *Langmuir* **1997**, *13*, 6480−6484.

(41) Als-Nielsen, J. *Physica A* **1986**, *140a*, 376−389.

(42) Braslau, A. B.; Pershan, P. S.; Swislow, G.; Ocko, B. M.; Als-Nielsen, J. *Phys. Rev. A* **1988**, *38*, 2457.

(43) Tidswell, I. M.; Ocko, B. M.; Pershan, P. S.; Wasserman, S. R.; Whitesides, G. M.; Axe, J. D. *Phys. Rev. B: Condens. Matter* **1990**, *41*, 1111−1128.

(44) Daillant, J.; Gibaud, A. *X-ray and neutron reflectivity: principles and applications*; Springer: Berlin, 1999.

(45) Tolan, M. *X-ray Scattering from soft-matter thin films: materials science and basic research*; Springer: Berlin, 1999; Vol. 148.

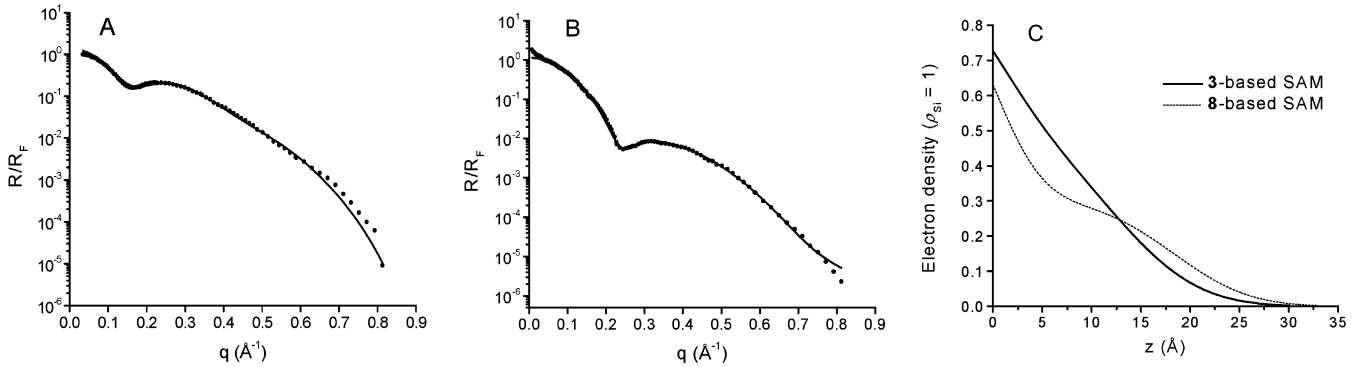

Figure 3. X-ray reflectivity of (A) a **3**-based monolayer and (B) an **8**-based monolayer; (C) a comparison between the electron density of the **3-** and **8**-based monolayers as a function of distance.

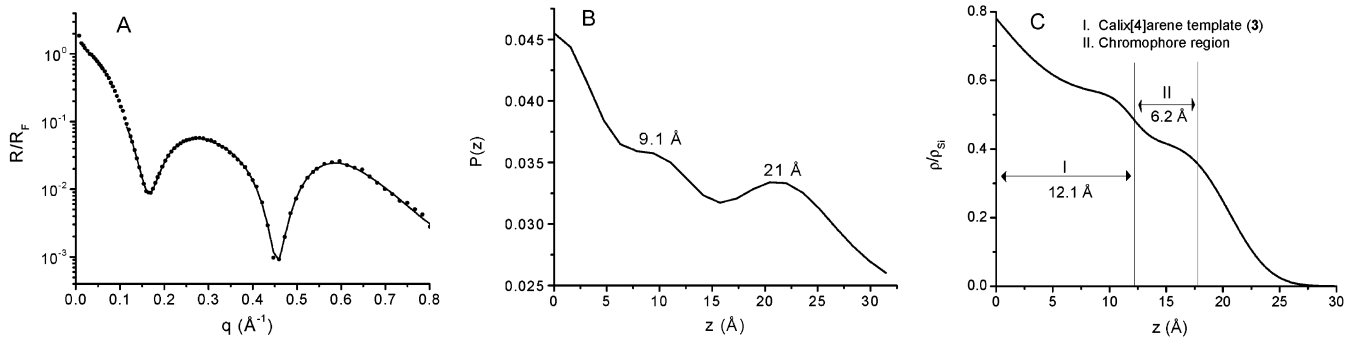

Figure 4. X-ray reflectivity measurements on a **3**,**11**-mixed SAM: (A) XRR data; (B) Patterson function for the same film; (C) electron density as a function of distance for the same film.

data were fitted to such a model, the fitting parameters being the thickness of each layer, the electron density of each layer, and the root-mean-square width of each interface. It should be noted that eq 3 is valid for q greater than approximately twice the critical wave vector for total external reflection ($q_c = 0.0316$ Å^{-1} for silicon), where refraction effects are negligible. Thus, the fits were performed using only data for which $q > 2q_c$.

Figure 3A,B shows normalized reflectivity data (R/R_F) from **3** and **8**-based films. The corresponding one-dimensional Patterson functions calculated from XRR data show only the large primary maximum due to the substrate−film and film−air interfaces. Solid lines in Figure 3A,B show best fits assuming a uniform electron density film with error-function-broadened interfaces. The XRR measurements on **3** and **8**-based monolayers reveal (i) a film thickness of 12.1 ± 0.5 Å (**3**) and 18.3 ± 0.7 Å (**8**), (ii) a film−air roughness of ∼6.9 Å (**3**) and ∼6.0 Å (**8**), and a film−substrate roughness of ∼4.6 Å (**3**) and ∼4.0 Å (**8**), respectively, and (iii) a molecular surface density of 120 ± 10 Å^2/molecule (8.7×10^{13} molecules/cm^2) (**3**) and 190 ± 10 Å^2/molecule (5.3×10^{13} molecules/cm^2) (**8**). The average alkyl-siloxane surface density of the calix[4]arene-based SAMs ∼35 Å^2/molecule (**3**) and ∼55 Å^2/molecule (**8**) is reasonable considering that the average molecular surface density of highly organized alkylsiloxane-based monolayers is ∼20−25 Å^2/molecule.[46−49] XRR analysis in combination with MM+ force-field calculations[50] indicate an average molecular tilt angle of ∼45° (**3**) and ∼50° (**8**) from the surface normal. The electron density profile obtained from fitting the reflectivity curve shows that the **3**-based film is more uniform than the **8**-based film (Figure 3C). The electron density profile for the latter can be divided into two regions: a region near the Si substrate with relatively high electron density and a second region with a lower density. The origin of such electron density profiles can be easily understood when one considers that the chemical structure of the **8**-based film consists of the calix[4]arene **3** (region 1) with a thickness of ∼12.1 Å and a chromophore layer (region 2) with a thickness of ∼6.2 Å.

Figure 4A shows the XRR data for the mixed 3,11-based film. The corresponding Patterson function is presented in Figure 4B. The large primary maximum at 21 Å is due to the substrate−film and film−air interfaces and its position indicates the overall thickness of the film. The existence of a secondary maximum at ∼9 Å in the Patterson function shows, without any model-dependent assumptions, that there is a clear density variation inside the film. Assuming the presence of two different regions with different electron densities within the film, we have obtained good fit to our data (solid line in Figure 4A). The first region, the calix[4]-arene layer **3**, has a thickness of 12.0 Å and an electron density, ρ, of ∼0.40 e Å^{-2}. The second region, the chromophore layer, has a thickness of 8.6 Å and $\rho \sim$ 0.30 e Å^{-2}. The interfacial and surface roughness, ∼1.4 and ∼2.8 Å, respectively, are less than the Si(111) substrate roughness, $\sigma_{si-film} \sim$ 4.5 Å. The film is

(46) Richter, A. G.; Durbin, M. K.; Yu, C.-J.; Dutta, P. *Langmuir* **1998**, *14*, 5980−5983.
(47) Whitesides, G. M.; Laibinis, P. E. *Langmuir* **1990**, *6*, 87−96.
(48) Tidswell, I. M.; Rabedeau, T. A.; Pershan, P. S.; Kosowsky, S. D.; Folkers, J. P.; Whitesides, G. M. *J. Chem. Phys.* **1991**, *95*, 2854−2861.
(49) Banga, R.; Yarwood, J.; Morgan, A. M.; Evans, B.; Kells, J. *Langmuir* **1995**, *11*, 4393−4399.
(50) MM+ calculations were performed using HyperChem(TM), Hypercube, Inc., 1115 NW 1114th Street, Gainesville, FL 32601, USA.

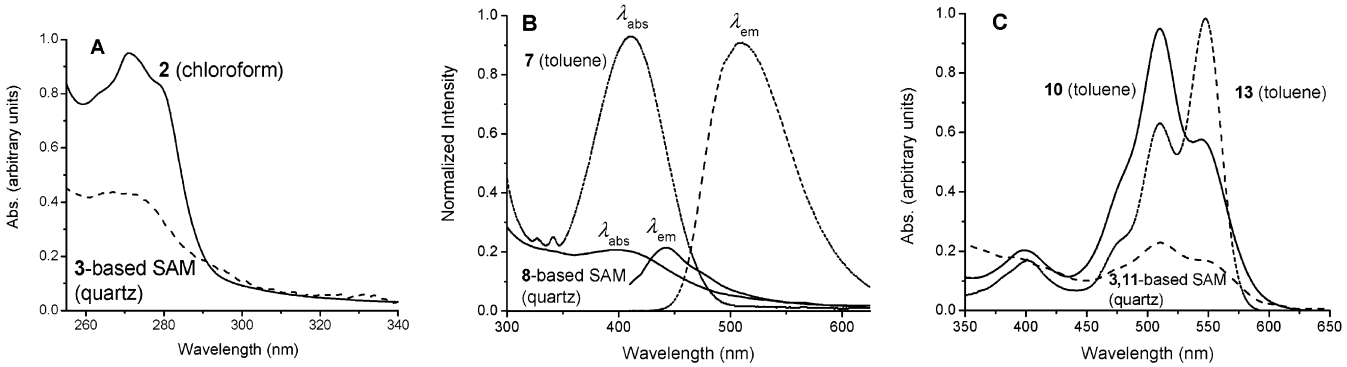

Figure 5. Optical absorption and fluorescence spectra in solution and in the solid state.

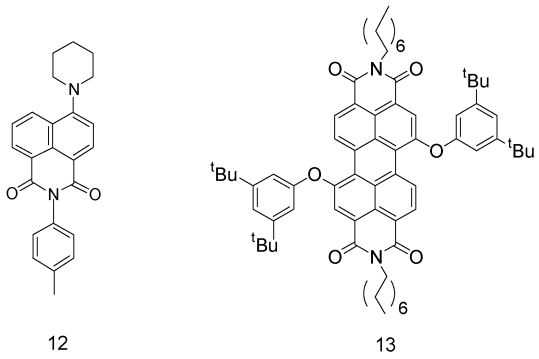

Figure 6. Structures of reference chromophores, **12** and **13**.

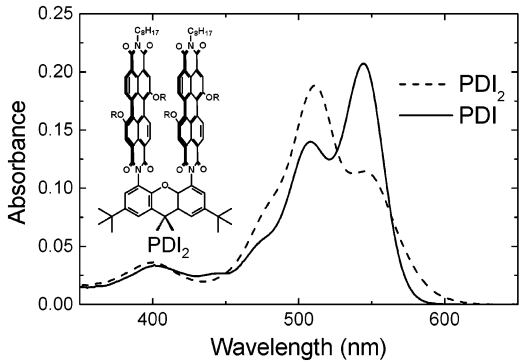

Figure 7. Optical absorption spectra of PDI and PDI_2 in toluene. R = 3,5-di-*tert*-butylphenyl.

remarkably smooth considering the fact that it consists of two bulky components (**3**, **11**) with entirely different molecular dimensions. The "molecular footprints" for the two regions, ∼120 and ∼280 Å^2/molecule, indicate that the ratio between **3** and **11** is about 1:1 on the surface. The average XRR-derived film roughness and surface densities of **3**, **8**, and the mixed **3**,**11**-based SAMs are comparable, arguing that the overall film structure is largely dictated by the calix[4]arene template and not by the chromophores.

Photophysical Properties of the Functionalized Calix[4]arene Films. The optical absorption spectrum of **3** shows a broad absorption band at 270 nm on quartz, which is similar to the absorption of precursor **2** in toluene (Figure 5A). The spectrum of **8** on quartz (Figure 5B) exhibits a band at 400 nm, similar to that of **7** in CH_2Cl_2. This band is a charge transfer (CT) transition characteristic of 4-aminonaphthalene-1,8-dicarboximide (ANI) chromophores.[51,52] Excitation of the **8**-based film at 400 nm results in fluorescence emission at 444 nm, which is blue-shifted by 56 nm relative to that of compound **7** in toluene. The CT nature of the lowest excited singlet state of the ANI chromophore results in its emission spectrum being solvatochromic.[51] The blue-shifted emission in the solid film strongly suggests that the polarity of the environment surrounding the ANI chromophore in the film is very low. Moreover, the close correspondence of the absorption spectra of **7** in solution and the **8**-based film to the spectrum of reference molecule **12** (Figure 6) suggests that the ANI molecules within the **8**-based film do not interact strongly with one another.

The optical absorption spectrum of the mixed **3**,**11** film resembles those of its precursors **2** and **10** in solution (Figure 5C). The absorbance of the calix[4]arene at 270 nm both in solution and in the solid state is obscured by the intense transitions of **10** and **11**. In sharp contrast to **7** and **8**, calix[4]arenes **10** and **11** exhibit distinctively different spectroscopic properties relative to those of the chromophoric monomer reference molecule *N*,*N*-(di-*n*-octyl)-1,7-(3,5-di-*tert*-butylphenoxy)-perylene-3,4:9,10-bis(dicarboximide), **13** (PDI) (Figure 6). For **10** and **11**, the absorption band at 550 nm is diminished relative to that of **13**, while a new band at 511 nm appears. Fluorescence measurements on **10** and **11** (not shown) show strong quenching of the 575-nm fluorescence emission characteristic of reference monomer **13**, and the appearance of a new, weaker emission band ($\phi_F \cong 0.1$) at 710 nm. The differences between the spectroscopic properties of reference molecule **13** and those of **10** and **11** are due to exciton coupling of the transition moments of the two PDI chromophores in **10** and **11**.

We have observed very similar behavior when two PDI chromophores are constrained by a diaminoxanthene spacer molecule[53] to a parallel, stacked geometry, which places the transition dipoles for the 550-nm transitions in the PDI chromophores parallel to one another (Figure 7).[54−56] Face-to-face stacking of an infinite number of chromophores will increase the

(51) Greenfield, S. R.; Svec, W. A.; Gosztola, D.; Wasielewski, M. R. *J. Am. Chem. Soc.* **1996**, *118*, 6767−6777.
(52) Miller, S. E.; Lukas, A. S.; Marsh, E.; Bushard, P.; Wasielewski, M. R. *J. Am. Chem. Soc.* **2000**, *122*, 7802−7810.
(53) Hamann, B. C.; Branda, N. R.; J. Rebek, J. *Tetrahedron Lett.* **1993**, *34*, 6837−6840.
(54) Langhals, H.; Ismael, R. *Eur. J. Org. Chem.* **1998**, 1915−1917.
(55) Langhals, H.; Jona, W. *Angew. Chem., Int. Ed.* **1998**, *37*, 952−955.
(56) Rohr, U.; Schlichting, P.; Böhm, A.; Gross, M.; Meerholz, K.; Bräuchle, C.; Müllen, K. *Angew. Chem., Int. Ed.* **1998**, *37*, 1434−1437.

exciton splitting by no more than a factor of 2 beyond that of the dimer, but this increase will be masked somewhat by the broad bandwidth of the transitions.[57] A comparison of the optical absorption spectra of PDI and PDI_2 in Figure 7 shows that PDI_2 exhibits a new, intense band at 511 nm, which agrees well with the predictions of the molecular exciton model. However, the optical transition from the ground state of PDI_2 to the lower exciton state, which is symmetry-forbidden in the molecular exciton model for the dimer geometry enforced by the xanthene spacer in PDI_2, still has significant oscillator strength as evidenced by the intensity of the band at 550 nm. Extension of the simple molecular exciton model to include vibronic coupling in the exciton states of the dimer relieves the symmetry restrictions inherent to the simple model.[58,59] Thus, the 511-nm band is the transition from the ground state to the $v = 0$ vibronic level of the upper exciton state, while the 550-nm band is the corresponding transition to the $v = 1$ vibronic level of the lower exciton state. The greater oscillator strength of the 511-nm transition in PDI_2 is consistent with the geometry of the dimer enforced by the xanthene spacer.

Conclusions

Calix[4]arene scaffolds can be used to position two photoactive molecules in a well-defined spatial relationship relative to one another, while at the same time allowing this unit to be positioned on flat, hydrophilic oxide surfaces. This strategy is particularly important when the function of the overall unit depends on the distance between the two photoactive molecules. Optical, AFM, and XRR measurements show that the bichromophoric calix[4]arenes form structurally regular, dense organic films. In addition, we have shown that two PDI molecules interact electronically when they are attached to the calix[4]arene upper rim at the 1- and 3-position. These interactions form dimers that maintain their interactions within the films. Despite the increased flexibility of the calix[4]arene scaffold, the two PDI molecules self-associate strongly. The results suggest that the calix[4]arene templated method may be suitable self-assembly of photofunctional arrays of a wide range of similar arylenebis(dicarboximide) chromophores for molecular electronic and photoconversion applications.

Experimental Section

General Methods. $H_2Pt(IV)Cl_6 \cdot xH_2O$, imidazole, piperidine, $HSi(OCH_3)_3$, and 4-bromo-1,8-naphthalic anhydride were purchased from Aldrich. 4-Bromo-1,8-naphthalic anhydride was purified by recrystallization from acetic anhydride. Acetic acid, nitric acid, Whatman PTFE, 0.45-μm pore size syringe filters were purchased from Fisher. 25,26,27,28-Tetrakis-(undecyleneoxy)calix[4]arene, **2**, was prepared according to literature procedures.[60] Toluene and CH_2Cl_2 were dried and distilled over CaH_2. ^1H NMR spectra were recorded on a Varian 400-MHz instrument; chemical shifts (δ) are reported in ppm and are referenced to residual solvent. The UV−vis spectra were recorded on a 1601PC Shimadzu spectrometer. Fluorescence emission spectra were obtained with a PTI QM-1 photon-counting fluorimeter. Advancing aqueous contact angles (CA) were measured on a standard tensiometric bench fitted with a Telfon micrometer syringe at room temperature. All reported CA values are the average of at least five measurements.

X-ray reflectivity measurements were performed at Beam Line X23B of the National Synchrotron Light Source at Brookhaven National Laboratory in Upton, NY, using a Huber four-circle diffractometer in the specular reflection mode (i.e., incident angle is equal to exit angle). X-rays of energy $E = 9.653$ keV ($\lambda = 1.28$ Å) were used for these measurements. The beam size was 0.35 mm vertically and 2 mm horizontally. The samples were placed under helium during the measurements to reduce the background scattering from the ambient gas and radiation damage. The experiments were performed at room temperature. The off-specular background was measured and subtracted from the specular counts. Details of the data acquisition and analysis procedure were reported previously.[30,46,61,62]

Atomic force microscopy was performed by using a Digital Instruments Multimode Nanoscope IIIa. All measurements were obtained in contact mode with oxide-sharpened silicon nitride (DNP-S20) Nanoprobe SPM tips.

Synthesis. *5,17-Dinitro-25,26,27,28-tetrakis(undecyleneoxy)-calix[4]arene (**4**).* Aqueous nitric acid (70%, 8.9 mL, 0.14 mol) was added dropwise to a solution of calix[4]arene (**2**; 2.0 g, 1.9 mmol) in CH_2Cl_2 (100 mL) and glacial acetic acid (17.8 mL). H_2O (50 mL) was added after the reaction mixture was stirred vigorously for 5 h under N_2. The organic layer was washed with H_2O until neutral pH, dried over $MgSO_4$, and concentrated. Column chromatography (hexane:ethyl acetate = 95:5 v/v) yielded **4** as a white powder (20%). ^1H NMR ($CDCl_3$, 400 MHz): δ 7.43 (s, 4H, *o*-Ar(NO_2)H), 6.74 (s, 6H, ArH), 5.81 (m, 4H, *CH*═CH_2), 4.97 (vt, 8H, CH═*CH*$_2$), 4.46 (d, 4H, $J = 13.8$ Hz, $ArCH_2Ar$), 3.92 (m, 8H, OCH_2), 3.26 (d, 4H, $J = 13.5$ Hz, $ArCH_2Ar$), 2.05 (m, 8H, OCH_2CH_2), 1.90 (m, 8H, CH_2CH═), 1.32 (s, 48H, CH_2). MS (EI): *m*/*z* 1123.7647 [M + 1]. Calcd for $C_{72}H_{103}N_2O_8$: 1123.7709.

*5,17-Diamino-25,26,27,28-tetrakis(undecyleneoxy)calix[4]-arene (**5**).* An ethanolic solution (10 mL) of **4** (0.24 g, 0.22 mmol) and $SnCl_2 \cdot 2H_2O$ (0.49 g, 2.2 mmol) was refluxed for 18 h. The solution attained room temperature and was poured into ice/water (~5 mL), and aqueous KOH (1.0 M) was added until pH > 8. The resulting solution was extracted with CH_2Cl_2 (4 × 10 mL) and the organic layer was washed with brine (4 × 5 mL) and dried over $MgSO_4$. After filtration, the solvent was evaporated, yielding product **5** as a white solid (95%). ^1H NMR ($CDCl_3$, 400 MHz): δ 6.87 (d, 4H, $J = 7.2$ Hz, ArH), 6.75 (m, 2H, ArH), 5.85 (s, 4H, ArH), 5.77 (m, 4H, *CH*═CH_2), 4.95 (ABq, 8H, $J = 24.6$ Hz, CH═*CH*$_2$), 4.36 (d, 4H, $J = 13.6$ Hz, $ArCH_2$-Ar), 4.05 (br, s, 4H, NH_2), 3.88 (t, 4H, $J = 7.6$ Hz, OCH_2), 3.69 (t, 4H, $J = 6.8$ Hz, OCH_2), 3.05 (d, 4H, $J = 13.2$ Hz, $ArCH_2$-Ar), 2.03 (m, 8H, OCH_2CH_2), 1.84 (m, 8H, CH_2CH═), 1.29 (s, 48H, CH_2). MALDI-MS: *m*/*z* 1062.8 [M]. Calcd for $C_{72}H_{106}N_2O_4$: 1062.8.

*Compound **7**.* 4-Bromo-1,8-naphthalic anhydride was added (55 mg, 0.20 mmol) to a solution of **5** (0.11 g, 0.10 mmol) in $CHCl_3$ (5 mL) and imidazole (27 mg, 0.40 mmol). The reaction mixture was refluxed for 5 h under N_2. The solvent was evaporated and **6** was obtained by column chromatography (CH_2Cl_2:hexane = 7:3 v/v). MALDI-MS: *m*/*z* 1585.1 [M + 4H]. Calcd for $C_{96}H_{112}Br_2N_2O_8$: 1581.7. A pyridine solution (7 mL) of **6** and piperidine (0.1 mL, 1.0 mmol) was refluxed for 3 h. The product **7** was obtained by column chromatography (CH_2Cl_2:hexane = 7:3 v/v), yielding a yellow powder (30%). ^1H NMR

(57) Kasha, M.; Rawls, H. R.; El-Bayoumi, M. A. *Pure Appl. Chem.* **1965**, *11*, 371−392.
(58) Fulton, R. L.; Gouterman, M. *J. Chem. Phys.* **1964**, *41*, 2280−2286.
(59) Oddos-Marcel, L.; Madeore, F.; Bock, A.; Neher, D.; Ferencz, A.; Rengel, H.; Wegner, G.; Kryschi, C.; Trommsdorff, H. P. *J. Phys. Chem.* **1996**, *100*, 11850−11856.
(60) Vreekamp, R. H.; Verboom, W.; Reinhoudt, D. N. *Recl. Trav. Chim. Pays-Bas* **1996**, *115*, 363−370.
(61) Roscoe, S. B.; Kakkar, A. K.; Marks, T. J.; Malik, A.; Durbin, M. K.; Lin, W.; Wong, G. K.; Dutta, P. *Langmuir* **1996**, *12*, 4218−4223.
(62) Malik, A.; Lin, W.; Durbin, M. K.; Marks, T. J.; Dutta, P. *J. Chem. Phys.* **1997**, *107*, 645−652.

($CDCl_3$, 400 MHz): δ 8.65 (m, 4H, naphthalene), 8.46 (d, 2H, $J = 8$ Hz, naphthalene), 7.73 (t, 2H, $J = 7.6$ Hz, naphthalene), 7.24 (d, 2H, $J = 8$ Hz, naphthalene), 7.09 (s, 4H, ArH), 6.38 (t, 2H, $J = 7.6$ Hz, ArH), 6.24 (d, 4H, $J = 8$ Hz, ArH), 5.81 (m, 4H, CH═CH_2), 4.97 (m, 8H, CH═CH_2), 4.49 (d, 4H, $J = 13.6$ Hz, $ArCH_2Ar$), 4.14 (t, 4H, $J = 8$ Hz, OCH_2), 3.67 (t, 4H, $J = 6.4$ Hz, OCH_2), 3.28 (br, 8H, piperidine), 3.16 (d, 4H, $J = 13.2$ Hz, $ArCH_2Ar$), 2.05 (m, 8H, OCH_2CH_2), 1.9 (br, 8H, piperidine), 1.75 (br, 4H, piperidine), 1.83 (m, 8H, CH_2CH═), 1.33 (s, 48H, CH_2). UV−vis (CH_2Cl_2): $\lambda_{max} = 400$ nm, $\epsilon = 2.5 \times 10^4$, $\lambda_{em} = 500$ nm, $\Phi_F = 0.91$. MALDI-MS: *m*/*z* 1591.4 [M + H]. Calcd for $C_{106}H_{132}N_4O_8$: 1590.2.

*Compound **10***. Compound **9** was added (0.47 g, 0.52 mmol) to a solution of **5** (0.21 g, 0.20 mmol) in pyridine (10 mL) and imidazole (1.0 g, 14.7 mmol). The reaction mixture was refluxed for 36 h under N_2. The solvent was evaporated and the title compound **10** was obtained as a red powder (20%) by column chromatography (CH_2Cl_2:hexane = 4:6 v/v). ^{1}H NMR ($CDCl_3$, 400 MHz): δ 9.74 (br, 4H, perylene), 8.69 (brd, 4H, $J = 22$ Hz, perylene), 8.38 (br, 4H, perylene), 7.36 (s, 4H, di-*tert*-butylphenyl), 7.04 (s, 8H, di-*tert*-butylphenyl), 6.81 (s, 4H, ArH), 6.35 (br, 2H, ArH), 6.17 (br, 4H, ArH), 5.80 (m, 4H, CH═CH_2), 4.96 (m, 8H, CH═CH_2), 4.47 (d, 4H, $J = 13.2$ Hz, $ArCH_2$-Ar), 4.13 (br, 8H, OCH_2), 3.77 (vd, 4H, $J = 6.0$ Hz, NCH_2), 3.15 (d, 4H, $J = 13.2$ Hz, $ArCH_2Ar$), 2.05 (s, 8H, OCH_2CH_2), 1.53 (m, 8H, CH_2CH═), 1.47 (s, 4H, NCH_2CH_2), 1.33 (m, 120H, CH_2, t-Bu CH_3), 0.93 (m, 26H, aliphatic). MALDI-MS: *m*/*z* 2468 [M + H]. Calcd for $C_{160}H_{232}N_4O_{16}$: 2467.4.

*Compounds **3**, **8**, and **11***. A dry CH_2Cl_2 solution of **2**, **7**, or **10** (25 mM), 2−3 crystals of $H_2Pt(IV)Cl_6 \cdot xH_2O$, and $HSi(OCH_3)_3$ (160 equiv) was stirred in a sealed sidearm flask overnight at room temperature. Subsequently, all volatiles were removed by high vacuum. The residue was dissolved in dry toluene (20 mL) and filtered (45-μm pore size PTFE syringe filters) prior to surface attachment. For **3**: ^{1}H NMR ($CDCl_3$, 400 MHz): δ 6.58 (m, 12H, ArH), 4.43 (d, 4H, $J = 13.2$ Hz,-$ArCH_2Ar$), 3.86 (br, 8H, OCH_2), 3.56 (s, 36H, OCH_3), 3.13 (d, 4H, $J = 13.2$ Hz, $ArCH_2Ar$), 1.88 (br, 8H, OCH_2CH_2), 1.30 (s, 64H, CH_2), 0.64 (t, 8H, $J = 7.6$ Hz, CH_2Si). MALDI-MS: *m*/*z* 1524.8. Calcd for $C_{84}H_{144}O_{16}Si_4$: 1525.5. For **8**: ^{1}H NMR ($CDCl_3$, 400 MHz): δ 8.62 (m, 4H, naphthalene), 8.46 (d, 2H, $J = 8$ Hz, naphthalene), 7.73 (t, 2H, $J = 7.2$ Hz, naphthalene), 7.24 (d, 2H, $J = 8$ Hz, naphthalene), 7.09 (s, 4H, ArH), 6.38 (t, 2H, $J = 8$ Hz, ArH), 6.24 (d, 4H, $J = 7.6$ Hz, ArH), 4.49 (d, 4H, $J = 13.6$ Hz, $ArCH_2Ar$), 4.13 (m, 4H, OCH_2), 3.66 (m, 4H, OCH_2), 3.57 (s, 36H, OCH_3), 3.27 (br, 8H, piperidine), 3.16 (d, 4H, $J = 13.2$ Hz, $ArCH_2Ar$), 2.0−1.70 (m, 20H, OCH_2CH_2, piperidine), 1.28 (s, 64H, CH_2), 0.64 (m, 8H, CH_2Si). MALDI-MS: *m*/*z* 2083 [M + H]. Calcd for $C_{118}H_{172}N_4O_{20}Si_4$: 2082.1. For **11**: ^{1}H NMR ($CDCl_3$, 400 MHz): δ 9.74 (br, 4H, perylene), 8.69 (brd, 4H, $J = 22$ Hz, perylene), 8.38 (br, 4H, perylene), 7.36 (s, 4H, di-*tert*-butylphenyl), 7.04 (s, 8H, di-*tert*-butylphenyl), 6.81 (s, 4H, ArH), 6.35 (br, 2H, ArH), 6.17 (br, 4H, ArH), 4.47 (d, 4H, $J = 13.2$ Hz, $ArCH_2Ar$), 4.13 (br, 8H, OCH_2), 3.77 (vd, 4H, $J = 6.0$ Hz, NCH_2), 3.55 (s, 36H, OCH_3), 3.15 (d, 4H, $J = 13.2$ Hz, $ArCH_2Ar$), 2.05 (s, 8H, OCH_2CH_2), 1.47 (s, 4H, NCH_2CH_2), 1.33 (s, 136H, CH_2, t-Bu CH_3), 0.93 (m, 26H, aliphatic), 0.64 (m, 8H, CH_2Si). MALDI-MS: *m*/*z* 2960.6 [M + H]. Calcd for $C_{172}H_{272}N_4O_{28}Si_4$: 2959.4.

Substrate Preparation. Silicon wafers (Semiconductor Processing Company) and quartz (Chemglass) were cleaned by immersion in a freshly prepared "piranha" solution (concentrated H_2SO_4:H_2O_2 30% = 7:3 v/v) at 80 °C for at least 45 min. *Caution! This solution is an extremely strong oxidizing agent*. After cooling to room temperature, the slides were rinsed repeatedly with deionized (DI) water and subjected to an RCA-type cleaning procedure (H_2O:H_2O_2 30%:NH_4OH = 5:1:1 v/v/v), sonicated at room temperature for 45 min. The substrates were then rinsed with DI water and dried in an oven overnight at 115 °C.

Preparation of SAMs. *(a) **3** and **8**-Based SAMs.* The freshly cleaned substrates were placed in an oven-dried Schlenk-type reactor. A dry toluene solution (0.7−1 mM) of **3** or **8** was added and reacted for 12 h at 80 °C. The solution was allowed to attain room temperature and was transferred by a canulla. The functionalized substrates were washed twice with toluene, acetone, and methanol and sonicated with methanol for 3 min. The substrates were dried under a stream of N_2.

*(b) **3**,**11**-Mixed SAMs.* A dry CH_2Cl_2 solution (3 mL) of **3** and **11**, one crystal of $H_2Pt(IV)Cl_6 \cdot xH_2O$, and $HSi(OMe)_3$ (160 equiv) was stirred in a sealed sidearm flask at room temperature for 18 h. Subsequently, all volatiles were removed by high vacuum. The residue was dissolved in dry toluene (20 mL) and filtered (45-μm pore size PTFE syringe filters) prior to surface attachment; see *(a)*.

Acknowledgment. This work was supported by the National Science Foundation under Grants CHE-0102351 (M.R.W.) and DMR-9978597 (P.D.) and was performed at beamline X23B of the National Synchrotron Light Source, which is supported by the U.S. Department of Energy.

CM034247H